UDC669.14.018.8-194.57:539.52:621.98

Press Formability of High-Purity Ferritic Stainless Steel Sheets

Hidehiko Sumitomo*1 Toshio Tanoue*2

Abstract:

The press formability of high-purity ferritic stainless steel sheets was examined by a multi-stage cylindrical deep drawing test. The effects of mechanical properties on deep drawability and the characteristics of press forming techniques were studied. The results are summarized as follows: (1) The high-purity ferritic stainless steels can be arranged in order of decreasing deep drawability as follows: boron-added YUS 436S > boron-free YUS 436S, YUS 190 > SUS 304 >> SUS 430. The addition of boron is especially effective in preventing the cold work embrittlement of excessively formed parts. (2) For the mechanical property evaluation factors, the $\bar{r}$ value showed a relatively good correlation with the deep drawability. The other factors, or elongation, the n value, the Erichsen value and conical cup value, showed no clear-cut correlation with the deep drawability. (3) It is important that any multi-stage cylindrical deep drawing process should be designed to ensure metal flow from the flange to the center of the cylinder. The redrawing ratio of 0.86 produced good results for the high-purity ferritic stainless steels.

1. Introduction

In recent years, the progress of stainless steel melting technology has advanced high-purity steel refining technology markedly. As a result, sharp reductions in the typical impurity elements of carbon and nitrogen have become economically feasible on an industrial scale, making it possible to supply large amounts of high-purity ferritic stainless steels with improved intergranular corrosion resistance and weldability at reduced cost[1,2].

Particularly, the automobile industry has studied in detail the corrosion resistance of high-purity ferritic stainless steels mainly in the exhaust gas environment of exhaust system parts and is switching from hot-dip aluminum-coated carbon steel sheets to high-purity ferritic stainless steel sheets[3,4].

Reducing the carbon and nitrogen contents of ferritic stainless steels improves mechanical properties, such as ductility and toughness, as well as corrosion resistance[5,6]. In the press forming of complex-shaped parts, it is considered important that deep drawability indexes, such as elongation, the n value and the Lankford value ($\bar{r}$ value), should be as high as possible. High-purity ferritic stainless steels excel in these properties, too, and

*1 Technical Development Bureau

*2 Stainless Steel Plate & Sheet Sales Division

Table 1 Chemical compositions of steels (wt%)

Steel	C	Si	Mn	P	S	Ni	Cr	Mo	Ti	Nb	N	B
YUS 190	0.004	0.13	0.13	0.026	0.005	—	18.95	1.84	0.15	0.16	0.009	—
YUS 436S (B added)	0.005	0.11	0.10	0.028	0.002	—	17.23	1.19	0.17	—	0.009	0.0008
YUS 436S (B-free)	0.003	0.07	0.09	0.026	0.003	—	17.16	1.10	0.16	—	0.009	0.0001
YUS 409D	0.004	0.43	0.33	0.019	0.002	—	10.89	—	0.17	—	0.007	—
SUS 430	0.050	0.47	0.12	0.018	0.001	—	16.23	—	—	—	0.010	—
SUS 304	0.043	0.48	1.10	0.027	0.001	8.31	18.05	—	—	—	0.056	—

are expected to provide a level of deep drawability unobtainable with conventional steels. However, few reports have been published about concrete cases in which their press formability into complex and difficult shapes has been experimentally studied.

Here, the deep drawability of the high-purity ferritic stainless steels is compared with that of the general-purpose stainless steels SUS 430 and SUS 304 by using multi-stage cylindrical deep drawing tools, and the property factors and press forming techniques essential for improving the deep drawability of the high-purity ferritic stainless steels are studied.

2. Experimental Methods

2.1 Materials

Four high-purity steels, including heat-resistant steels, and SUS 430 and SUS 304 as controls were studied. The chemical compositions of these steels are listed in **Table 1**. The high-purity ferritic stainless steels have a combined carbon and nitrogen content of 140 ppm or less. The carbon and nitrogen are stabilized by titanium and niobium additions. Some have molybdenum additions of 1 to 2% to further raise corrosion resistance. YUS 436S has extra boron to improve cold work embrittlement. The effectiveness of the boron addition was verified in an experiment described later.

The high-purity ferritic stainless steels were melted through the basic oxygen furnace (BOF)-vacuum oxygen decarburization (VOD) route, continuously cast into slabs, hot-rolled, cold-rolled, final annealed, and skin passed at a mill. The high-purity ferritic stainless steels and the general-purpose stainless steels all cold-rolled to 0.6 mm thickness sheets.

2.2 Mechanical tests

JIS No.13B specimens were machined from each steel in parallel with the rolling direction and tension tested at a cross head speed of 5 mm/min. The n value of the specimens was calculated from the slope of their stress-strain curves at between 10 and 20% strains. JIS No.5 specimens were machined from the steels and elongated by 15% to determine their r value.

The Erichsen test and the conical cup test were performed to evaluate the formability of the steels. The Erichsen test was conducted by the method A specified in JIS Z 2247. Based on JIS Z 2249, the conical cup test was conducted by using Type 13 tools on 0.6-mm thick and 36-mm diameter blanks.

The hardness of the steels was measured at the midthickness by a Vickers hardness tester.

2.3 Deep drawing test

To evaluate their deep drawability, the steels were 20-stage cylindrical deep drawing tested in a 60-ton hydraulic press. A 144-mm diameter blank was punched and drawn into a cylinder at a ratio of 1.78 in the first stage. In the second and subsequent stages, the cylinder was redrawn at ratios of 0.80 to 0.93 (mainly 0.86) to the final shape illustrated in **Fig. 1**. The die profile radius was chiefly 6.0 mm, and the punch profile radius ranged from 7.0 to 0.8 mm. The dies and punches were made of SKD-11 alloy tool steel, and a commercial oil-base press forming lubricant was used.

To investigate the forming limit of the deep-drawn cylinders, their thickness strain and cross-sectional hardness were measured. When a cylinder cracked during deep drawing, its fracture surface was examined by scanning electron microscopy.

3. Experimental Results and Discussion

3.1 Mechanical properties

The tensile test results, hardness test results, and formability evaluation results for the steels are given in **Table 2**. The stress-strain curves of three typical steels are shown in **Fig. 2**.

Since their combined carbon and nitrogen content is held lower than that of the general-purpose ferritic stainless steel SUS 430, the high-purity ferritic stainless steels are lower in the 0.2% proof stress and longer in elongation. Their $\bar{r}$ value is greatly improved by their high purity. As a result, the Erichsen value and the conical cup value (CCV) are improved. The press forming of the austenitic stainless steel SUS 304 induces martensite transfor-

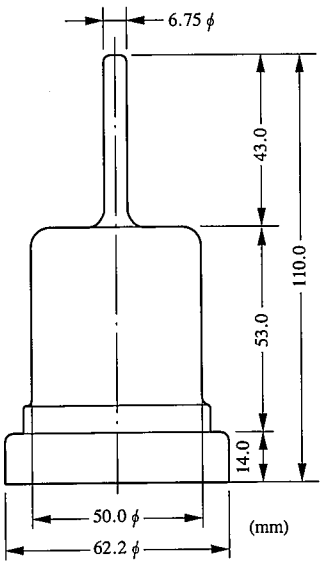

Fig. 1 Final shape of multi-stage deep-drawn cylinder

Table 2 Mechanical properties and press formability of steels

Steel	0.2% proof stress (N/mm²)	Tensile strength (N/mm²)	Elongation (%)	Hardness HV	n value	Lankford value				Erichsen value (mm)	Conical cup value (mm)
						r_0	r_{45}	r_{90}	$\bar{r}$		
YUS 190	343	497	33.8	173	0.20	1.60	1.47	2.10	1.66	9.5	26.7
YUS 436S (B-added)	275	459	34.8	135	0.21	1.67	1.63	2.12	1.76	9.8	26.9
YUS 436S (B-free)	284	483	34.5	137	0.22	1.49	1.90	2.01	1.83	9.8	26.8
YUS 409D	239	424	37.2	116	0.24	1.51	1.77	2.11	1.79	9.7	26.7
SUS 430	308	472	31.8	159	0.21	0.94	0.92	1.50	1.07	8.9	28.5
SUS 304	281	705	64.0	172	0.44	0.91	1.19	0.83	1.03	12.5	27.0

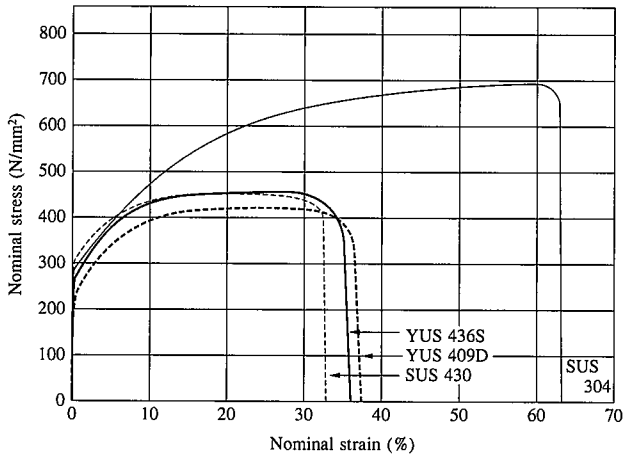

Fig. 2 Stress-strain curves

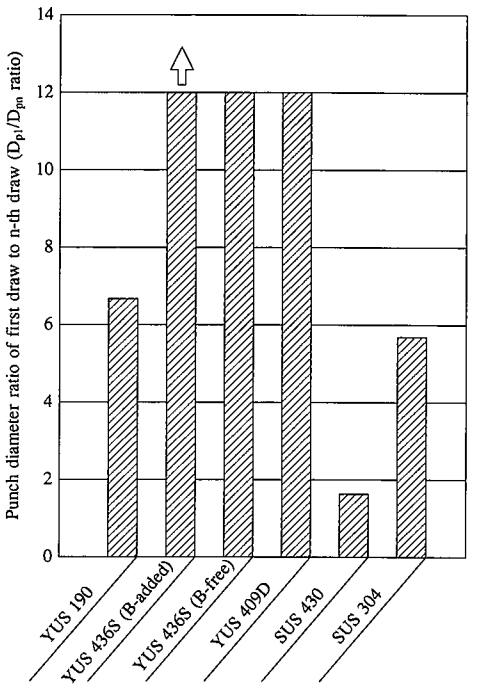

Fig. 3 Deep drawability as determined by multi-stage deep drawing test

mation and accentuates the work hardening of deformed portions. These tendencies facilitate strain dispersion, increase the n value, and make the elongation and Erichsen value extremely high.

3.2 Deep drawability as determined by multi-stage cylindrical drawing

The deep drawability of the steels as determined by multi-stage cylindrical drawing is evaluated by the punch diameter ratio of the first draw to the n-th draw (D_{p1}/D_{pn}) and shown in **Fig. 3**.

The multi-stage deep drawability of the high-purity ferritic stainless steels is by far higher than that of the general-purpose stainless steels SUS 430 and SUS 304. In particular, boron-added YUS 436S can be redrawn in 20 or more stages. As a result, the punch diameter in the n-th stage can be reduced to 1/12 or less of that in the first stage, and cylinders can be formed to a drawing ratio that varies in inverse proportion to the punch diameter reduction ratio. By making the diameter of the blank as the reference, this effect is converted into the total drawing ratio of 21.3. This means that the high-purity ferritic stainless steels can be continuously deep drawn in multi-stages without intermediate annealing of complex parts. These are difficult to deep draw with general-purpose stainless steels and require intermediate annealing. **Photo 1** shows a part deep drawn from a high-purity ferritic stainless steel in 20 stages.

Boron-free YUS 436S and YUS 409D fractured in the 20th stage. This fracture was a longitudinal crack propagating in the drawing direction and is different from a crack near the punch profile radius for SUS 430 and SUS 304 or what is called an α fracture. The above-mentioned results show that the experimental

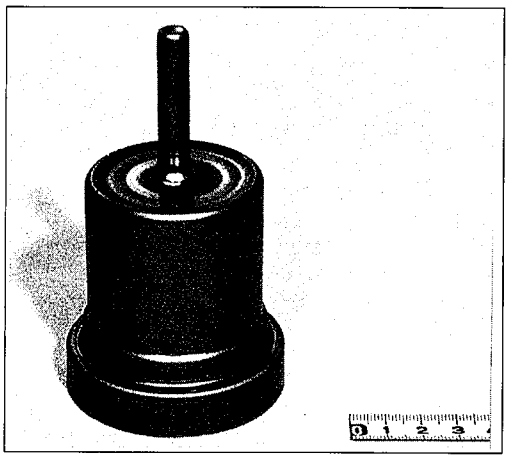

Photo 1 Press-formed part

steels can be arranged in decreasing order of multi-stage cylindrical deep drawing performance as follows: boron-added YUS 436S > boron-free YUS 436S, YUS 409D > YUS 190 > SUS 304 >> SUS 430.

3.3 Effects of mechanical properties on multi-stage deep drawing performance

To grasp the multi-stage deep drawing performance of the high-purity ferritic stainless steels, including the general-purpose ferritic and austenitic stainless steels, their relationship with the mechanical properties listed in **Table 2** was studied. The study results are shown in **Fig. 4**.

The deep drawability of the ferritic stainless steels improves as their elongation, n value, and Erichsen value increase, but the ranges over which the latter properties vary are extremely narrow. When the austenitic stainless steels are included, the correlation of deep drawability with elongation, n value, and Erichsen value is not necessarily clear. Of the mechanical properties studied, the $\bar{r}$ value exhibited a relatively high correlation with the multi-stage deep drawability as pointed out by Goto et al.[7] The CCV correlates slightly with the multi-stage deep drawability when evaluated on a macrobasis for all the steels studied. The range over which the high-purity ferritic stainless steels' CCV varies is so narrow that their CCV does not show a clear-cut correlation with their multi-stage deep drawability.

Generally, high formability is expected of steels of high n value in view of forming strain dispersion. The n value is particularly effective for stretching[8] and as pointed out by Hayakawa et al.[9] should be considerably low for deep drawing, such as multi-stage cylindrical drawing.

3.4 Effect of boron on formability of high-purity ferritic stainless steels

Extra-low-carbon steels (interstitial-atom free or IF steels) have extremely low carbon and nitrogen contents and have the amount of solute carbon reduced to the lowest possible limit by adding suitable amounts of titanium and niobium singly or in combination. The IF steels are susceptible to grain-boundary embrittlement and likely to experience cold work embrittlement in deep drawing[10]. Boron is known as an element effective in improving the cold work embrittlement of the IF steels[11]. The authors confirmed the effectiveness of boron in improving the cold work embrittlement of some high-purity ferritic stainless steels that have the same crystal structure as that of the IF steels[12]. Boron was added in trace amounts of 8 ppm to YUS 436S, and its effectiveness was verified by the multi-stage drawing test.

High-r-value YUS 436S and YUS 409D, irrespective of boron level, exhibited high deep drawability to the 19th stage. Without added boron, these steels developed longitudinal cracks

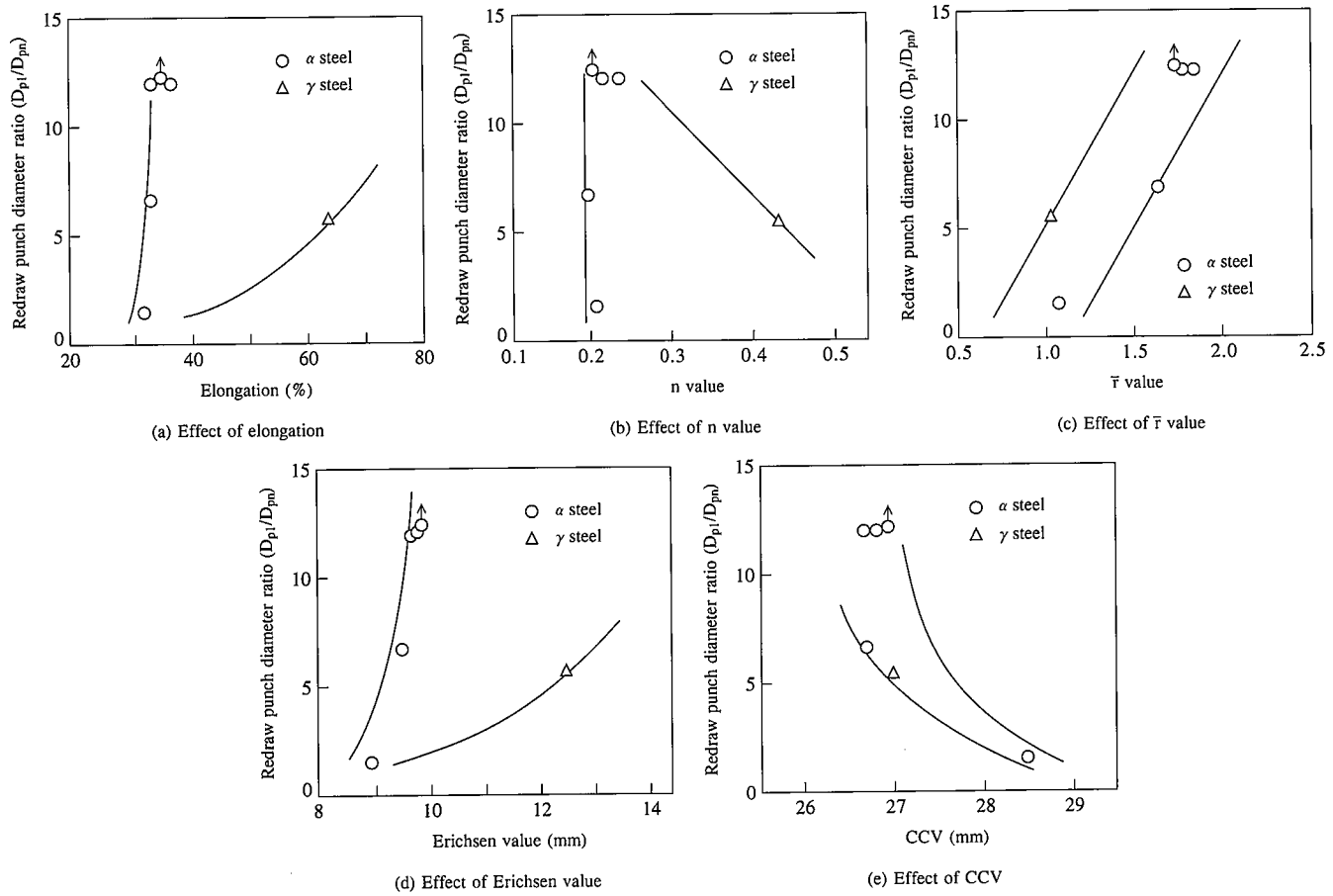

(a) Effect of elongation
(b) Effect of n value
(c) Effect of $\bar{r}$ value
(d) Effect of Erichsen value
(e) Effect of CCV

Fig. 4 Effects of mechanical properties on multi-stage cylindrical drawing performance

when expanding stress acted at the cylinder edge in the 20th stage. On the other hand, YUS 436S containing 8 ppm of boron exhibited no such fracture and was successfully formed into the target shape.

A longitudinal fracture surface of boron-free YUS 436S and a conventional α fracture surface of SUS 430 are compared in **Photo 2**. The fracture surface of SUS 430 exhibited a conventional dimple fracture pattern due to the ductile forming limit, while the longitudinal crack of boron-free YUS 436S exhibited an intergranular fracture surface. It is well-known that IF steels exhibit this type of intergranular fracture pattern on the fracture surfaces of cold work embrittlement[13] and this agrees well with this result.

These results indicate the possibility that adding boron to the YUS 409D that developed the longitudinal crack in the 20th deep drawing stage may provide it with the same deep drawability as exhibited by YUS 436S.

3.5 Deformation and work hardening by multi-stage deep drawing

Fig. 5 shows the changes in the thickness strain and hardness of parts deep drawn in the 20th stage from the YUS 436S steels that exhibited the best deep drawability.

The thickness strain decreased by 25% at the punch profile radius (r_{p1}) of the tip of the cylinder in the center, rapidly increased in the edge direction of the cylinder, returned to the original level at 18 mm from the center, and increased by a maximum of 42% just before the first die profile radius (r_{d1}). The thickness strain then decreased from the first die profile radius (r_{d1}) to the punch profile radius (r_{p2}) at the outside of the cylinder, followed the original level between r_{p2} and r_{p4}, and increased again at the edge of the cylinder. The thickness strain changed in this complex manner. The boron addition exerted no appreciable effect on the thickness strain.

Compared with the complicated thickness changes noted above, the hardness changed relatively monotonically and measured about 230 to 270 HV in the side wall of the cylinder, except at the center. As described above, the thickness strain was close to 0% between the positions r_{p2} and r_{p4}. When estimated from the cold reduction-induced hardness shown in **Fig. 6**, the thickness strain of nearly 0% corresponds to a cold reduction of about 50%. This is probably the result of the increase in the thickness

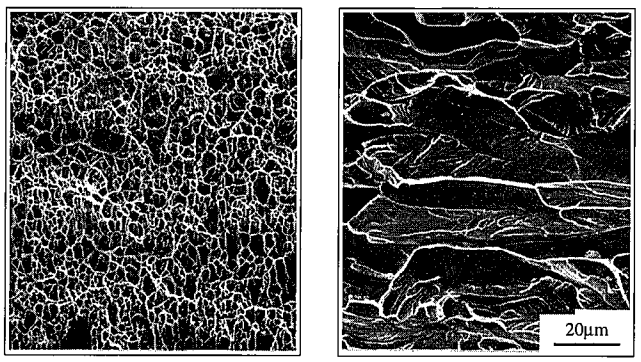

(a)SUS 430 (drawn to 5th stage)

(b) YUS 436S without B addition (drawn to 20th stage)

Photo 2 Fractographs produced by scanning electron microscopy

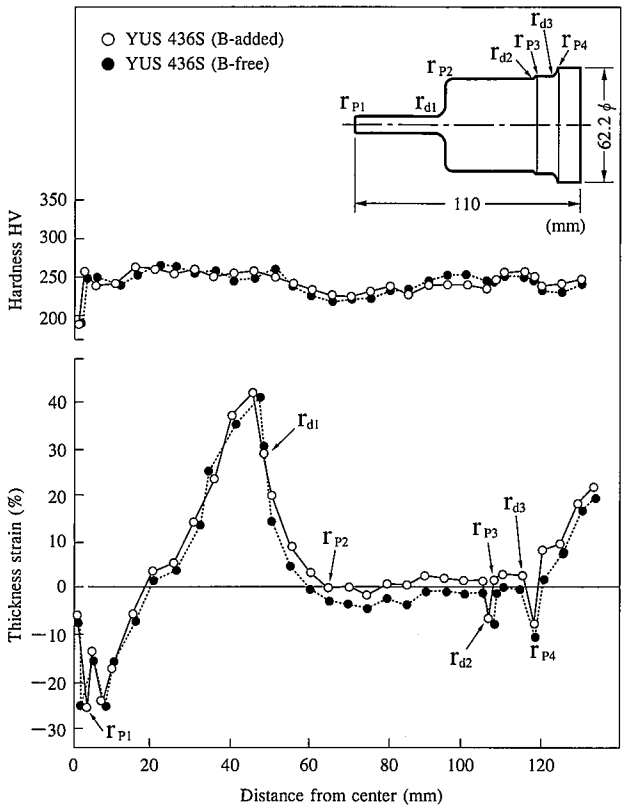

Fig. 5 Changes in thickness strain and hardness of cylinders press formed in multi-stages from YUS 436S

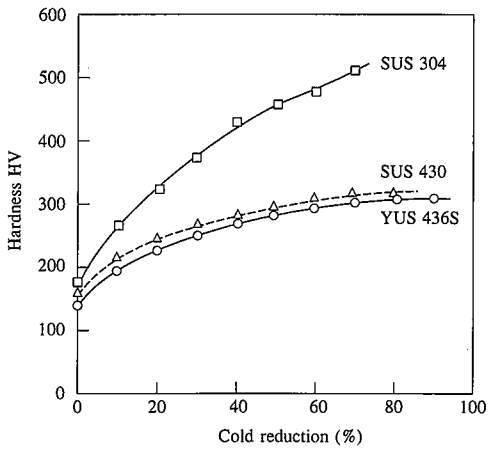

Fig. 6 Effect of cold reduction on hardness

of the metal flow from the edge of the cylinder being offset by the decrease in the thickness of the metal flow in the drawing direction.

The thickness increase in the side wall of the cylinder and the progress of drawing deformation with the original thickness retained suggest that the metal flow from the flange was greater than required to compensate for the decrease in the thickness. The rise in the depth was due to the increasing number of drawing stages. In other words, multi-stage drawing tools should be designed to set these redrawing ratios and punch and die profile radii that permit this type of metal flow. Under the experimental conditions of the present study, good results were obtained with the redrawing ratio of 0.86 for the high-purity ferritic stainless steels.

The change in the thickness strain of a SUS 430 cylinder that cracked in the 5th drawing stage is shown in comparison with a YUS 436S cylinder in **Fig. 7**. As compared with YUS 436S, SUS 430 with a smaller $\bar{r}$ value was more likely to decrease in thickness locally, become necked near the punch profile radius of the cylinder at the center, resulting in an α fracture there.

The changes in the thickness strain and hardness of a SUS 304 cylinder that cracked in the 14th drawing stage are shown in comparison with a YUS 436S cylinder in **Fig. 8**. Compared with YUS 436S, SUS 304 had a minute increase in thickness at the center of the cylinder and had a greater rise in thickness at the edge of the cylinder. It had a hardness of 350 to 450 HV and generally exhibited high work hardening. SUS 304 is characterized by the change in hardness from the center to the edge of the cylinder. In particular, its hardness peaked at two positions, r_{d1} and r_{d3}.

From these results, the cylindrical drawing behavior of SUS 304 with a high n value may be considered as follows. The first draw sharply raised the hardness of the edge of the cylinder and delayed metal flow to the center of the cylinder in the second and subsequent drawing stages. As a result, plane, strain-type deformation was concentrated at the punch tip and caused the cylinder to fracture at the r_{p1} portion.

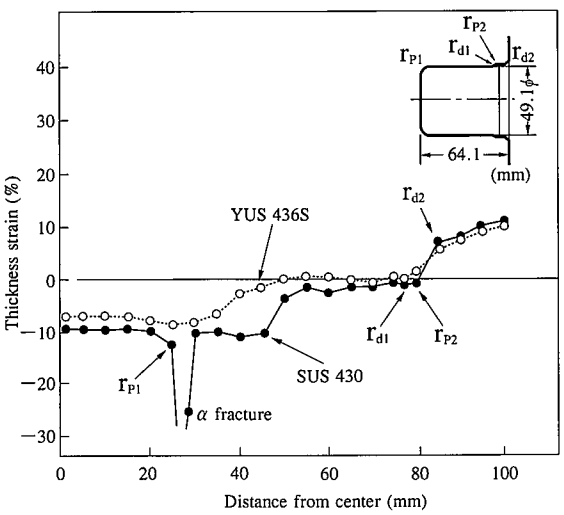

Fig. 7 Changes in thickness strain of cylinders press formed in the 5th drawing stage from SUS 430 and YUS 436S

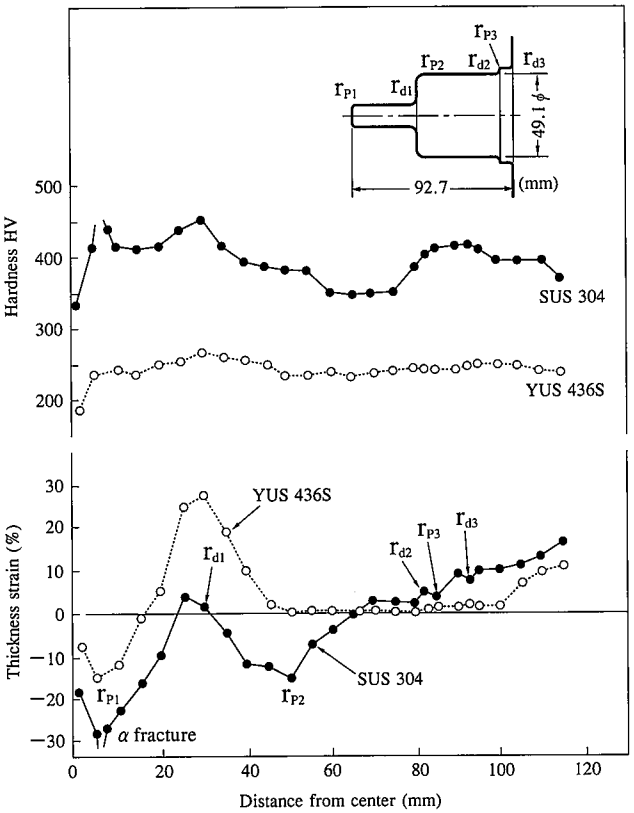

Fig. 8 Changes in thickness strain of cylinders press formed in the 14th drawing stage from SUS 430 and YUS 436S

This finding suggests that the multi-stage cylindrical deep drawing of SUS 304 should be designed to set the drawing ratio in the first drawing stage as small as possible and to reduce the punch diameter difference in the second and subsequent drawing stages.

4. Conclusions

The press formability of high-purity ferritic stainless steel sheets was evaluated by a 20-stage cylindrical deep drawing test. The effects of mechanical properties on deep drawability and the characteristics of press forming techniques were studied. The following findings were obtained:

(1)The high-purity ferritic stainless steels were confirmed to decrease in deep drawability in the following order: boron-added YUS 436S > boron-free YUS 436S, YUS 409D > YUS 190 > SUS 304 >> SUS 430.

(2)The high-purity ferritic stainless steels are likely to undergo cold work embrittlement when excessively formed, but this tendency can be improved by adding trace boron.

(3)Of the steel property factors that indicate formability, the $\bar{r}$ value showed a relatively good correlation with deep drawability. The other factors, or the elongation, n value, Erichsen value, and CCV showed no clear-cut correlation with the deep drawability.

(4)In the multi-stage deep drawing of cylinders, preventing the wall thickness of the cylinder at the center from decreasing is important in preventing the α fracture of the cylinder. The redrawing ratio, die profile radius, and punch profile radius

should be set to facilitate the metal flow from the flange to the center of the cylinder. Under the experimental conditions of this study, the redrawing ratio of 0.86 provided good results for the high-purity ferritic stainless steels.

Acknowledgments

The authors are indebted to Hiroaki Sakurai of Kyosan Denki Co., Ltd. and others for their cooperation in the deep drawing test of the steels.

References

1) Hasegawa, M.: Stainless Steel Handbook. Third Edition. Nikkan Kogyo Shimbun, 1995, p. 775
2) Tsujino, R. et al.: Shinnittetsu Giho. (351), 35 (1993)
3) Ishikawa, H.: Nishiyama Memorial Seminar, ISIJ. 1994, p. 2554
4) Sato, E. et al.: Shinnittetsu Giho. (354), 11 (1994)
5) Sawatani, T. et al.: Tetsu-to-Hagané. 63 (5), 832 (1977)
6) Binder, W.O. et al.: Trans. ASM. 43, 759 (1951)
7) Goto, Y. et al.: Proceedings of the 45th Japanese Joint Conference for the Technology of Plasticity. 1994, p. 319
8) Sumitomo, H. et al.: Proceedings of the 1976 Japanese Spring Conference for the Technology of Plasticity. 1976, p. 151
9) Hayakawa, H. et al.: CAMP-ISIJ. 8, 704 (1995)
10) Shimizu, M.: Doctoral dissertation "Study on Development of Extra-Deep Drawing Quality Cold-Rolled Steel Sheet". 1972, Kyoto University
11) Takahashi, N. et al.: Proc. of Conf. on Metallurgy of Continuous-Annealed Sheet Steel. AIME, 1982, p. 133
12) Fudanoki, F. et al.: Tetsu-to-Hagané. 73 (5), 143 (1987)
13) Yamada, M. et al.: Tetsu-to-Hagané. 73 (8), 1049 (1987)